**Atmospheric
Chemistry
and Physics
Discussions**

This discussion paper is/has been under review for the journal Atmospheric Chemistry and Physics (ACP). Please refer to the corresponding final paper in ACP if available.

Preliminary estimation of black carbon deposition from Nepal Climate Observatory-Pyramid data and its possible impact on snow albedo changes over Himalayan glaciers during the pre-monsoon season

T. J. Yasunari[1,2], P. Bonasoni[3,4], P. Laj[5], K. Fujita[6], E. Vuillermoz[4], A. Marinoni[3], P. Cristofanelli[3], R. Duchi[3], G. Tartari[7], and K.-M. Lau[1]

[1]NASA Goddard Space Flight Center, Greenbelt, USA
[2]Goddard Earth Science and Technology Center, University of Maryland Baltimore County, Baltimore, Maryland, USA
[3]CNR – Institute for Atmospheric Sciences and Climate, Bologna, Italy
[4]Ev-K2-CNR Committee, Bergamo, Italy
[5]Laboratoire de Glaciologie et Géophysique de l'Environnement, Université Grenoble 1 – CNRS (UMR5183), St. Martin d'Heres, France

Title Page

Abstract | Introduction

Conclusions | References

Tables | Figures

◄◄ | ►►

◄ | ►

Back | Close

Full Screen / Esc

Printer-friendly Version

Interactive Discussion

[6]Graduate School of Environmental Studies, Nagoya University, Japan
[7]CNR – Water Research Institute, Brugherio (Mi), Italy

Correspondence to: T. J. Yasunari (teppei.j.yasunari@nasa.gov)

Estimated lower
bound BC deposition
over Himalayas

T. J. Yasunari et al.

Title Page

Abstract	Introduction
Conclusions	References
Tables	Figures

|◄ | ►|

◄ | ►

Back | Close

Full Screen / Esc

Printer-friendly Version

Interactive Discussion

T. J. Yasunari et al.

Abstract

The possible minimal range of reduction in snow surface albedo due to dry deposition of black carbon (BC) in the pre-monsoon period (March–May) was estimated as a lower bound together with the estimation of its accuracy, based on atmospheric observations at the Nepal Climate Observatory-Pyramid (NCO-P) sited at 5079 m a.s.l. in the Himalayan region. We estimated a total BC deposition rate of 2.89 µg m^{-2} day^{-1} providing a total deposition of 266 µg m^{-2} for March–May at the site, based on a calculation with a minimal deposition velocity of 1.0×10^{-4} m s^{-1} with atmospheric data of equivalent BC concentration. Main BC size at NCO-P site was determined as 103.1–669.8 nm by correlation analysis between equivalent BC concentration and particulate size distribution in the atmosphere. We also estimated BC deposition from the size distribution data and found that 8.7% of the estimated dry deposition corresponds to the estimated BC deposition from equivalent BC concentration data. If all the BC is deposited uniformly on the top 2-cm pure snow, the corresponding BC concentration is 26.0–68.2 µg kg^{-1} assuming snow density variations of 195–512 kg m^{-3} of Yala Glacier close to NCO-P site. Such a concentration of BC in snow could result in 2.0–5.2% albedo reductions. From a simple numerical calculations and if assuming these albedo reductions continue throughout the year, this would lead to a runoff increases of 70–204 mm of water drainage equivalent of 11.6–33.9% of the annual discharge of a typical Tibetan glacier. Our estimates of BC concentration in snow surface for pre-monsoon season can be considered comparable to those at similar altitude in the Himalayan region, where glaciers and perpetual snow region starts in the vicinity of NCO-P. Our estimates from only BC are likely to represent a lower bound for snow albedo reductions, since a fixed slower deposition velocity was used and atmospheric wind and turbulence effects, snow aging, dust deposition, and snow albedo feedbacks were not considered. This study represents the first investigation about BC deposition on snow from atmospheric aerosol data in Himalayas and related albedo effect is especially the first track at the southern slope of Himalayas.

Printer-friendly Version

Interactive Discussion

1 Introduction

Atmospheric aerosol is an important forcing for the earth's climate through direct and indirect effects (IPCC, 2007). Aerosols generally scatter solar radiation, but black carbon (BC), and mineral dust absorb to a lesser extent solar radiation. Long range transport of BC and dust are well known (e.g., Hadley et al., 2007; Yasunari et al., 2009; Uno et al., 2009). Due to their large amounts present in the Atmospheric Brown Cloud (Ramanathan et al., 2007), these absorbing aerosols may directly warm the atmosphere in the Indian-monsoon region. Lau et al. (2006, 2008), proposed the so-called *Elevated Heat Pump* (EHP) effect, whereby heating of the atmosphere by elevated absorbing aerosols strengthens local atmospheric circulation, leading to a northward shift of the monsoon rain belt, with increased rainfall in northern Indian and the foothills of the Himalayas in the late boreal spring and early summer season. More recently, Lau et al. (2010) showed that the EHP effect can also lead to accelerated melting of snow cover in the Himalayas and Tibetan Plateau, by a transfer of energy from the upper troposphere to the land surface over Tibetan Plateau. In addition, BC and mineral dust depositions onto snow-surface in the cryosphere may reduce the surface albedo (e.g., Warren and Wiscombe, 1980; Aoki et al., 2006, 2007; Tanikawa et al., 2009). The impurity effect on snow albedo reduction is more important for visible wavelength than that for near infrared radiation (e.g., Warren and Wiscombe, 1980; Flanner et al., 2007). It increases heating of the snow and ice surface, thus accelerating melting, shortening snow duration, and altering mass balance and causing retreat of mountain glaciers, which change the amount of available water resource in the region (e.g., Hansen and Nazarenko, 2004; IPCC, 2007; Flanner et al., 2007, 2009).

The southern slope of the Himalaya is directly exposed to Indian emissions and more likely to be impacted by BC than the northern slope. However, the available data of BC deposition (BCD) for studying snow albedo reduction at the southern slopes in Himalayan regions are still very scarce. Moreover, only a few BC concentrations (BCC) and morphological properties in snow and ice core in the northern slopes of the

Estimated lower bound BC deposition over Himalayas

T. J. Yasunari et al.

Himalaya and Tibetan Plateau region have been measured thus far (Xu et al., 2006, 2009a, b; Ming et al., 2008, 2009; Cong et al., 2009, 2010). Studies on BC concentration in snowpack at the southern slope in Himalayas are few compared to those at northern slopes. In addition, glaciers in Himalayas are located in severe topography and logistics constraints have severely limited data availability on snow and ice composition, as well as atmospheric composition observations. Hence, an alternative approach to estimate BCD over Himalayan glaciers is necessary for understanding impact of BCD on melting glaciers.

Atmospheric data of equivalent BC concentration (eqBCC), aerosol particle number concentration and size distribution, as well as meteorological parameters are now continuously measured at the Nepal Climate Observatory-Pyramid (NCO-P, 5079 a.s.l.) on Southern slope of the Himalayans (Bonasoni et al., 2008, 2010) (Fig. 1). The NCO-P is the highest aerosol observatory managed within the Ev-K2-CNR "SHARE" (Stations at High Altitude for Research on the Environment) and UNEP "ABC" (Atmospheric Brown Clouds) projects. This station was established in March 2006 for atmospheric research in the Khumbu Valley, Sagarmatha National Park, near the base of the Nepalese side of Mt. Everest (5079 m a.s.l.) (http://evk2.isac.cnr.it/). Since high altitude measurement sites are relatively clean and far from anthropogenic emission sources, they can be considered to study the influence of anthropogenic pollution transported from remote areas.

The Indian sub-continent, especially the Indo-Gangetic Plain is one of the largest BC emission sources in the world (Ramanathan et al., 2007) and it is in the vicinity of the Himalayan glaciers. Preliminary work of Bonasoni et al. (2008) has found very elevated eqBCC under different meteorological conditions, with well defined seasonality showing a maximum in pre-monsoon season (Marinoni et al., 2010). The aim of this study is to provide a preliminary lower bound estimate of BCD and BCC on and in the snow surface on the Himalayan region during the pre-monsoon period, based on NCO-P atmospheric observations recorded in March–May 2006. Basing on the estimated BCC in snow surface, we compute the possible minimal snow albedo reduction range and

Estimated lower bound BC deposition over Himalayas

T. J. Yasunari et al.

the related additional snow melt runoff from a typical Tibetan glacier by simple numerical calculations with a glacier mass balance model. These estimations are the first step of a study finalized to carry out more precise estimations on snow albedos and snow melt runoffs from glaciers using regional model, satellite, and more detailed observations in Himalayan regions, including seasonal variations of atmospheric concentration and deposition of absorbing aerosols. Hopefully, this study will stimulate more work on albedo reduction and accompanied snow melt runoff from glaciers over Himalayan region.

In this study, a BC concentration range in the snow surface due to the minimal deposition of BC onto snow surface will be estimated by using NCO-P data with typical snow density data over a Himalayan glacier (Sect. 3.2) with the discussion on possible dilution and enrichment effect of BCC in snow by precipitation and sublimation (Sect. 3.3). The snow albedo reduction will be assessed based on an empirical relationship between snow albedo reduction rate and BCC in snow (Ming et al., 2009) in Sect. 3.4. The possible deviation range as error from our estimated snow albedo reductions will be also discussed in Sect. 3.5. Finally, we will calculate how much the estimated albedo reductions can possibly impact on the increase of snow melt runoff from glaciers. Here we carried out some numerical experiments with a glacier mass balance model for a typical Tibetan glacier in Sect. 3.6, in which we assumed continuous albedo reductions throughout the year.

2 Data and method to estimate BC deposition

With the purpose of estimating the lower bound of snow surface albedo reductions at a typical Himalayan glacier due to BCD, we first calculate BCC in snow surface by a fixed slower deposition velocity together with atmospheric measurements conducted at the NCO-P (Bonasoni et al., 2008, 2010): meteorological parameters (temperature, pressure, relative humidity, wind intensity, wind direction, and rain) at 30 min interval (VAISALA WXT510); number concentrations and size distribution of aerosol with op-

tical diameter between 0.25 and 32 µm in 31 size channels, on 30 min interval (OPC, optical particle counter, GRIMM#190) and eqBCC (MAAP, Multi-Angle Absorption Photometer, 5012) in the atmosphere on 30 min interval, were recorded. A recommended mass absorption coefficient of 6.6 g m^{-2} was used for calculating BC concentration
[5] (Petzold et al., 2002). Additional information on MAAP measurements and calibration procedures are shown by Marinoni et al. (2010). Particles with mobility diameter between 10.31 and 669.8 nm were determined in 117 ranges (whole size range is 3.035–995 nm, but data in 10.31–669.8 nm were only available and used) by Scanning Mobility Particle Sizer (SMPS) on 1 h interval. Inlet of all these measurements was
[10] placed at 3.5 m above ground level (a.g.l.). As a first step, we determined the main BC particle size and estimate the amount of BCD onto snow surface during pre-monsoon season 2006 from the eqBCC, OPC number concentration, and SMPS size distribution data observed at the NCO-P. With the aim of determining the main particle size range of atmospheric eqBC, we carried out correlation analyses between the number counts
[15] in each diameter bin of OPC and SMPS and eqBCC in the air. In cases of unavailable data at a specific time, the whole set of necessary data on calculation were deleted. We used the middle time of the averaged observation slot time for plotting data.

Next, with the aim of calculating minimal BCD flux at the surface, here we consider a deposition velocity. The estimated BCD flux will be used to estimate BCC in snow sur-
[20] face and its impact on snow surface albedo reductions. As deposition velocity, here, we consider a constant minimal deposition velocity of 1.0×10^{-4} m s^{-1}. In general, detailed deposition velocity is considered as:

$$v_d = 1/(r_a + r_b + r_c) + v_s \tag{1}$$

where r_a, r_b, r_c, and v_s are aerodynamic resistance above canopy, quasi-laminar
[25] layer resistance, surface resistance, and terminal velocity by gravitational settling, respectively (Han et al., 2004). Deposition velocity is higher over land than over sea and the deposition velocities in different particle size over land are mostly faster than 1.0×10^{-4} m s^{-1} (Nho-Kim et al., 2004). Hence, our deposition velocity used in this

study will be expected as a slower value than deposition velocities in general diurnal cycles over land and considered as lower bound deposition velocity, minimal value, of deposition velocity.

Using the minimal deposition velocity, the 1-hourly total amount of BC deposition rate will be then accumulated over the three-month period to obtain the total mass of BC deposited on snow surface.

3   Results and discussions

3.1   Determination of BC size range and deposition rate

While the MAAP instrument specifically measures the aerosol absorption coefficient, directly related to BCC, both the OPC and SMPS measures total aerosol number concentration and size distributions of all aerosol components including BC. To ascertain the typical size range of BC, the correlation analyses between counts in OPC and SMPS bins and eqBCC in the atmosphere were carried out in time series data (Fig. 2a and b). Higher correlation coefficients (more than 0.8) were seen in the ranges 280–650 nm for OPC-eqBCC and 103.1–669.8 nm for SMPS-eqBCC, respectively. This confirms that the BC particles at NCO-P preferably have sizes ranging between 100 and 670 nm, as indicated by the high correlation between eqBCC and PM_1 showed by Marinoni et al. (2010). The MAAP measures BCC as eqBCC in the atmosphere, since Marinoni et al. (2010) found the negligible dust contribution to aerosol absorption coefficient at NCO-P. In order to reduce any miscounting due to absorbing organic carbon we chose significantly higher correlations ($r > 0.8$) as BC particle existence. In fact, previous study (Venzac et al., 2008) found much smaller particles (10–20 nm growing up to 40 nm) possibly related to the mode of new particle formation from gaseous or ionic precursors at this site , while larger fraction (>600 nm) of submicron particles is generally present at low concentrations.

Estimated lower bound BC deposition over Himalayas

T. J. Yasunari et al.

Title Page

Abstract   Introduction

Conclusions   References

Tables   Figures

|◄   ►|

◄   ►

Back   Close

Full Screen / Esc

Printer-friendly Version

Interactive Discussion

Less precipitation has been observed in Khumbu valley during pre-monsoon season (Bollasina et al., 2002; Bonasoni et al., 2008, 2010). As deduced by NCO-P data (Bonasoni et al., 2008, 2010), in the high Khumbu valley during March–May 2006, precipitation events were only 1.9% of all the available meteorological data during March–May 2006 and the total precipitation amount was very low (6.9 mm). Hence, it is reasonable to assume that the main cause for BC removal in the atmosphere in this season was due to dry deposition.

The minimal BC dry deposition flux at the surface was estimated from MAAP and SMPS data, separately. Because enough observation instruments are not always available for field observations, we should consider some ways to estimate BCD from limited observations. At the NCO-P site, eqBCC and SMPS are now available and here we consider two types of BCD estimations. First, the total BC mass deposition flux per 1 h was calculated using eqBCC data from MAAP as (eqBCC)×(the minimal deposition velocity of $1.0\times10^{-4}\,\mathrm{m\,s^{-1}}$)×(interval time=3600 s). We summated the BC flux for March–May and obtained total deposition amount of BC of $266\,\mu\mathrm{g\,m^{-2}}$ (=$2.89\,\mu\mathrm{g\,m^{-2}\,day^{-1}}$). Then, we also estimated total dry deposition flux per 1 h from SMPS data as $\sum$(BC mass concentration in each size bin)×(the minimal deposition velocity of $1.0\times10^{-4}\,\mathrm{m\,s^{-1}}$ for each size bin)×(interval time=3600 s). In the calculation, we assumed uniform BCC in the atmospheric layer from the ground to the measurement height of 3.5 m a.g.l. and BC continuously depositing onto the surface. The mass concentrations in the atmosphere in each size bin were calculated from SMPS data, considering spherical particles with a reference particle density (here we used a BC density of $2000\,\mathrm{kg\,m^{-3}}$ by Lindstedt, 1994). It is because the SMPS covers wider range of particle size than that of OPC for the small particles, and the correlations between eqBCC, and OPC – SMPS counts gives similar results as shown in Fig. 2a and b, except for the smaller diameters that are not available by this instrument. The interval of SMPS data was 1 h and continuous depositions during this interval were assumed. The values of dlogD in each bin were used for converting size distribution data (dN/dlogD) to number concentration data. Then total dry deposition amount of

3059 μg m^{-2} was obtained for the period of March–May. The SMPS data include more aerosol information than MAAP and this deposition amount may include not only BC but also other aerosol particles. If we compare the total dry deposition amount from SMPS with the total BC deposition amount of 266 μg m^{-2} from MAAP, the estimated BC deposition amount from MAAP is 8.7% of the total dry deposition amount from SMPS. This is somewhat consistent with the observed mass contribution of Elemental Carbon in aerosol at NCO-P (Decesari et al., 2009) and soot abundance at Mt. Qomolangma (Everest) (Cong et al., 2010). Hence, we considered that approximately 8.7% of total dry deposition amount from SMPS data is likely composed of BC at NCO-P site. Then, 1-hourly dry deposition amount from SMPS data was converted to 1-hourly BCD amount multiplied by a coefficient of 0.087. The estimated BCD from MAAP was mainly used for the discussions on BC concentrations in snow and related albedo reductions.

Although MAAP and SMPS were different observations, the variations of the estimated BCD from SMPS data were superimposed on the atmospheric eqBCC from MAAP (Fig. 3a; red). It indicates that the 1-hourly BCD amount estimated from SMPS data with the coefficient of 0.087 for the particle size range of 103.1–669.8 nm was well explained by eqBCC variations in the atmosphere. The large variability in Fig. 3a is mostly driven by diurnal cycles of BCD. The diurnal cycle shows clearly a midnight-morning low and an afternoon high BCD rates, consistent with the diurnal cycle of dry convection in this region during the pre-monsoon periods (Fig. 3b). The same diurnal cycle was seen for aerosol scattering and absorption coefficients at NCO-P site (Marcq et al., 2010). A few acute episode of BC pollution has been observed in this period (eqBCC exceeded some thousand of ng m^{-3}), leading to an estimated dry deposition of BC larger than 1 μg m^{-2} h^{-1}. Although we used a fixed deposition velocity as a considered minimal value for the estimated BCD amount, expected faster deposition velocity in actual will likely increase our estimated BCD rate.

3.2 Estimation of BC concentration in surface snow

The total mass of BC deposited on the surface during 2006 pre-monsoon season was estimated as the sum of the BCD integrated the 3-month period with available data. Based on this, we obtained a total BCD amount of $266\,\mu g\,m^{-2}$ for the pre-monsoon season, corresponding to $2.89\,\mu g\,m^{-2}\,day^{-1}$. As indicated in Sect. 3.1, most likely, this value represents the lowest line of the actual BCD. Most of the glaciers in Nepal generally exist above the altitude of the NCO-P while their ablation basin levels are close to its altitude (Karma et al., 2003). Most of the glacier melting occurs in ablation areas. The equilibrium line altitudes of these glaciers are also above the NCO-P level. Hence, our discussion from the estimated BCD can be applicable to the ablation zone of these glaciers.

The 2-cm top layer (5-cm top layer in Aoki et al., 2000) of snow surface is more contaminated than the deeper part of the snow layer because the snow impurities are derived from direct depositions of atmospheric aerosols (Aoki et al., 2000, 2007; Tanikawa et al., 2009). Moreover, the surface layer contributes to a large fraction of the semi-infinite albedo in snow contaminated by soot and mineral dust (Tanikawa et al., 2009). In addition, Tanikawa et al. (2009) showed that the mass concentration of snow impurities deposited in the surface layer of ∼2 cm was about 30–50 ppmw whereas that deposited in 2–10 cm was about 2–6 ppmw. This characteristic between surface layer and lower snow layer was seen for elemental carbon, organic carbon, and dust in their study. It indicates that the impurity concentration at the top 2-cm is much more higher than that below 2 cm and the top snow layer is considered to be the key to assess albedo reductions. Hence, our focus on 2-cm snow surface is reasonable for albedo reduction calculations as a preliminary estimate.

To calculate the BCC in the top layer of snow, we assumed that the total BC is uniformly distributed in the top 2 cm pure snow. Since BCC is strongly depends on snow water content and since no data on snow density are available for NCO-P area, we used observed surface snow density data at the nearby Yala Glacier by Fujita et

al. (1998) (Table 1). The glacier is located in the Nepalese Langtang Valley (28.23° N; 85.60° E; 2.5 km^2, between 5094–5749 m of altitude) about 123 km away the NCO-P and at very similar altitude (Fig. 1). A pure snow layer extension deeper than 2 cm can significantly increase the water amount, thus influencing our BCC estimates. However, a similar pure snow layer extension to the deeper later is not realistic based on the studies as mentioned above (Aoki et al., 2000, 2007; Tanikawa et al., 2009) and snow layers below 2 cm usually include impurities to some extent.

As the NCO-P altitude corresponds to the lowest elevation of Yala glacier, our estimated BCD can be considered to be applicable to the termini of glaciers at similar elevations in Nepal as reported in Karma et al. (2003). In that consideration, we also assume that transport along valleys and BC source strength can be similar to those at the high Kumbu valley. If the total BC of 266 µg m^{-2} deposited on 2-cm thickness of pure snow and without pre-existing or other contamination such as dust, BCC in the snow surface will vary within the range of 26.0–68.2 µg kg^{-1} due to snow density variations between 195–512 kg m^{-3} in Table 1. These estimated concentrations are in good agreement with BCC at other glaciers in the Himalayan region (Table 2). From Table 2, we also note that the upper limit of the NCO-P estimated BC snow concentration exceeds the values observed at other locations on the northern slope of the Himalayan range. In particular the East Rongbuk glacier, approximately 16 km to NCO-P but on the opposite side of Mt. Everest, shows the lowest BCC (Table 2). Ming et al. (2008) also found in the same East Rongbuk glacier area the highest level of BCC, 20.3±9.2 µg kg^{-1}, during the period 1995–2002, exceeding 50 µg kg^{-1} in the summer of 2001 along a significant increasing trend. Our results together with the mentioned studies suggest that the influence of strong polluted air masses transported from the Indo-Gangetic Plain and driven by valley breezes up to high mountain and glaciers, is very large on southern slope of the Himalayas (Bonasoni et al., 2008).

Estimated lower bound BC deposition over Himalayas

T. J. Yasunari et al.

Title Page

Abstract | Introduction

Conclusions | References

Tables | Figures

◄ | ►

◄ | ►

Back | Close

Full Screen / Esc

Printer-friendly Version

Interactive Discussion

3.3 Estimation of dilution effect at the snow surface on BC concentration

Precipitation onto snow surface dilutes BCC in snow; nevertheless pre-monsoon season is well known as dry season in South Asian region and low precipitation amount (6.9 mm) were observed at NCO-P during March–May 2006. Due to the dryness of the period, we expect that most of the aerosol fallout was due to dry deposition as mentioned in Sect. 3.1. For strengthen the discussion on BCC in snow without much dilution effect by precipitation during pre-monsoon season, we also examined the dilution effect on BCC in the snow surface. Assuming that there are not so much differences on precipitation amount between NCO-P site and Yala Glacier because of similar altitude and vicinity, we considered that precipitation at NCO-P are as same as that at Yala Glacier. Then, we assumed same precipitation amount over Yala Glacier. The air temperature over Yala Glacier was also estimated from NCO-P air temperature data (Fig. 4) with temperature lapse rate of $6.5 \, \mathrm{K \, km^{-1}}$. The air temperature at the altitude over Yala Glacier fell below freezing during most of the time in March–May (Fig. 4). Thus, most of the precipitations were expected as snowfall. When it snows, snow depth slightly increased with a typical fresh snow density of $110 \, \mathrm{kg \, m^{-3}}$. As deduced by NCO-P observation, the largest amount of precipitation occurred during 18:30–19:00 (30 min) on 18 May (Fig. 4). However, this could contribute to an increase of only 2 cm of snow depth by fresh snow (hereafter called, Event A). Total precipitation amount during March–May was only 6.9 mm w.e., indicating that the pre-monsoon is very dry in 2006 and most of the aerosol fallout was considered to be dry deposition as mentioned in Sect. 3.1. It is noted that the above example cannot be generalized for all the years, because there could be large interannual variability in pre-monsoon snowfall over this region.

For the sake of discussing dilution effect on BCC in snow by precipitation, we also calculated the evaporation amount (E) from the snow surface (sublimation if the snow surface temperature was below 0 degree in Celsius) every 30 min by using a bulk equation. In the calculation, air and snow surface temperature over Yala Glacier at altitude of

5450 m were used, where snow density data in Table 1 were obtained. For estimating snow surface temperature quantitatively, we need irradiance data. However, NCO-P site did not measure irradiance data during March–May 2006. Hence, we assumed snow surface temperature as −9, −4, and −1 degree in Celsius during 3/1–4/29, 4/30–5/23, and 5/24–5/31, respectively (Fig. 5), compared to the estimated air temperature over Yala Glacier in Figs. 4 and 5. In general, snow temperature fluctuations are much lower than that of air temperature. Based on the characteristics, our values of snow surface temperature are considered to be realistic.

Then, we calculated the evaporation (sublimation in this study) amount (E) by a bulk equation as follows:

$$E = \rho_{\mathrm{AIR}} C_H U (Q_{\mathrm{SAT}}(Ts) - \mathrm{RH} \times Q_{\mathrm{SAT}}(T_A)) \times DT \tag{2}$$

where ρ_{AIR}, C_H, U, $Q_{\mathrm{SAT}}(T_S)$, $Q_{\mathrm{SAT}}(T_A)$, RH and DT are air density, a bulk coefficient (=0.002), wind speed, saturated specific humidity at the snow surface, saturated specific humidity in the atmosphere, relative humidity in percentage divided by 100, and total time in second for 30 min (=1800 s). The fixed air pressure at the altitude of Yala Glacier was also used for this calculation. The direction from the snow surface to the atmosphere is defined as positive in the equation.

The difference between precipitation (P) and evaporation (E) (or sublimation) ($P - E$) shows the amount of water vapor transport between the snow surface and the atmosphere. In Fig. 5, the values of $P - E$ showed negative values over most of the pre-monsoon periods indicating dominant water vapor transport from the snow surface to the atmosphere. Hence, sublimation was likely prominent and dry condition continued during March–May 2006. Before Event A shown in Figs. 4 and 5b, total amount of $P - E$ was −23.6 mm w.e. and that after and including Event A, the amount was 3.6 mm w.e. Total amount of $P - E$ during March–May is −20.0 mm w.e. Bonasoni et al. (2010) mentioned that VAISALA can underestimate total precipitation due to the omission of snowfalls. However, even if we expect the total precipitation amount of 6.9 mm was 50% of the true value of total precipitation amount, still the water vapor

loss from snow surface was more dominant than precipitation. It implies that higher probability of enrichment of BC at the snow surface due to water loss from the snow surface is expected during March–May rather than the dilution effect by precipitation. Our estimates of BCC in 2-cm snow surface of 26.0–68.2 $\mu g\,kg^{-1}$ did not include the effect of this enrichment of BC due to the water loss from the snow surface. If we consider this effect, BCC in the snow surface during pre-monsoon period could be even higher. In conclusion, our estimates of BCC are considered to be "lower bound" values without including the enrichment effect of $P - E$.

3.4 Estimation of snow albedo reduction

To estimate the changes in snow surface albedos from the estimated total BCD of 266 $\mu g\,m^{-2}$ during March–May 2006, we used the linear regression equation ($R^2=0.9951$) by Ming et al. (2009):

$$\text{Snow\_albedo\_reduction} = 0.0757 \times \text{BCC} + 0.0575. \qquad (3)$$

This was obtained from the relationship between BCC in snow and potential albedo reductions, derived from a variety of snowpack observations and model calculations. For the given range of snow density and BCC in snow, we obtained the range of albedo reduction ranging from 2.0 to 5.2% during pre-monsoon period (Fig. 6). This range is significantly higher than the albedo reduction (1%) found by Grenfell et al. (1994) for a uniform distribution of 15 $\mu g\,kg^{-1}$ BC in snow, as indicated by the calculation of Warren and Wiscombe (1980). Flanner et al. (2007) indicated that the addition of 500 $\mu g\,kg^{-1}$ of BC to snow decreased its visible albedo approximately 10% in visible wavelengths, and calculated that the instantaneous forcing over the Tibetan Plateau, due to the presence of BC in snow, exceeds 20 Wm^{-2} in some places. Because snow aging process may also accelerate more BC accumulations onto snow surface (Xu et al., 2006), and because our BCD was determined only considering dry deposition, our numbers are likely to underestimate of the actual albedo reduction for Himalayan glaciers.

3.5 Estimation of the albedo in function of different type of snow age and BC

In reality, the albedo decrease caused by BC depends on a wider range of environmental factors such as snow grain size, solar zenith angle, and snow depth (e.g., Warren and Wiscombe, 1980). However, the application of using the regression Eq. (3) is probably adequate for a first estimate of albedo changes because our aim in this study is to determine the minimal level of possible albedo reductions due to BCD. Ice surface is sometimes come up over glacier surface, but the results obtained by using the Eq. (3) can be applied to the snow surface composed of fresh, compacted, and granular snows, in which the snow density range is similar to that of Yala glacier in Table 1.

The albedo reductions obtained from the regression equation by Ming et al. (2009) may provide lower bound of albedo reductions as mentioned in Sect. 3.4. However, the estimate of albedo reduction, in general, includes some errors and we need to estimate the possible deviation range in the estimation by using regression Eq. (3). The data used in this study were obtained from the Supporting Table 4 in Hansen and Nazarenko (2004) (see the website at: http://www.pnas.org/content/suppl/2003/12/15/2237157100.DC1/7157Table4.html), 2.3% albedo reduction by BCC of $25\,\mu g\,kg^{-1}$ by Jacobson (2004), 1% albedo reduction by BCC of $15\,\mu g\,kg^{-1}$ by Grenfell et al. (1994) with the model of Warren and Wiscombe (1980). The estimates of albedo reductions from observed BC concentrations in snow by Hansen and Nazarenko (2004) were based on Fig. 2 of Warren and Wiscombe (1985). Hence, the estimated albedo reductions are based on the calculation of the albedo model of Warren and Wiscombe (1985). They calculated the albedo reductions as external mixture case of BC for new and old snows and also mentioned the importance of internal mixture to explain true effect of soot. Therefore, in the study of Hansen and Nazarenko (2004), the estimate for internal mixing increased the BC absorption coefficient, or effective amount, by a factor of two along the descriptions by Warren and Wiscombe (1985). In the calculation of Warren and Wiscombe (1985), new and old snows are considered as the grain radius sizes of 0.1 mm and 1.0 mm, respectively. The meteorological con-

dition was expected as subarctic summer, clear sky, and solar zenith angle effect of 53° at sea level in their estimates. The albedo reduction rates were estimated at the wavelength of 470 nm in their calculation, at which snow albedo is most sensitive to soot content. Finally, Hansen and Nazarenko (2004) categorized BC and snow into 2
5 types of BC with 2 types of snow condition (4 types) as external mixture of BC with new snow (Ext/New), external mixture of BC with old snow (Ext/Old), internal mixture of BC with new snow (Int/New), and internal mixture of BC with old snow (Int/Old). Therefore, we used 2 types of BC with 2 types of snow condition and calculated each regression equation from the employed data with the estimated error (Fig. 7 and Table 3). The
10 data from Jacobson (2004) and Grenfell et al. (1994) with the model of Warren and Wiscombe (1980) were put into the categories of Int/New and Ext/New, respectively. The errors between the employed and estimated albedo reduction data from the regression equations are within approximately 1% (Table 3). There are large differences among the estimated albedo reductions by each type with each equation (Fig. 7a and
15 b). Warren and Wiscombe (1985) explained that a given amount of soot causes a greater reduction in albedo in old snow than in new snow because the radiation penetrates deeper on average in old coarse grained snow and therefore encounters more absorbing material before being scattered back out of the snowpack.

Most of the estimated values on albedo reduction by using the equation of Ming et
20 al. (2009) for BCC of 26.0–68.2 µg kg^{-1} were found within the range of those in Ext/New and Int/New (Fig. 7b). The snow albedo reduction for BCC of 68.2 µg kg^{-1} using the method of Ming et al. (2009) slightly exceeded the value by Int/New (Fig. 7b). Most of the estimated albedo reductions were located in the middle values of albedo reductions in new snow condition. Hence, the range of albedo reductions between Ext/New and
25 Int/New in Fig. 7b may correspond to the approximate errors in our estimation of albedo reductions. As mentioned in Fig. 4, there were much less precipitation event during pre-monsoon season in 2006 and the snow surface is considered to be old aged snow over Himalayan glaciers during most of the time in March–May. It also indicates that the snow surface albedo would probably reduce along the Ext/Old or Int/Old cases in

actual. If we use the equations of Ext/Old and Int/Old, much more albedo reductions are expected even if we only take BC into account. In those cases with Eqs. (2) and (4) in Table 3, the snow albedo for Ext/Old and Int/Old can possibly decrease by 4.6–11.0% and 7.2–16.5%, respectively (Table 4). These albedo reductions are significantly higher than those found using the equation by Ming et al. (2009) (2.0–5.2% albedo reductions). These results show that our estimate of albedo reduction is lower line.

3.6 Numerical experiment on albedo changes and increasing snow melt runoff

Lastly, we carried out numerical experiments to evaluate the influence of the albedo changes on glacier melting run-off from the Tibetan glacier with the glacier mass-balance-model by Fujita (2007) and Fujita et al. (2007). The model calculates the melt water, refrozen water, and runoff after solving for surface energy balance and heat conduction in the glacier ice. The snow surface albedo was calculated based on snow density in the model (Yamazaki et al., 1993). We currently do not have detailed input data on the model calculations for Himalayan glaciers. Hence, in this study, the numerical experiments were carried out for a typical Tibetan glacier in Fig. 1 (Dongkemadi Glacier: 33.07° N; 92.07° E; 14.63 km^2; 5275–5926 m a.s.l.) with the observed data by Fujita et al. (2007). As shown by Xu et al. (2006), the BCCs (elemental carbon in their case) over this glacier ranged from 18.2 to 168.2 µg kg^{-1} from snow pit works and the highest concentration was detected from a dirty layer. It indicates that Dongkemadi Glacier is also highly contaminated by seasonal BC depositions and can be considered to be suitable for our numerical experiments. The model calculated density-based snow albedos were always reduced by applying the albedo reductions of 2.0% or 5.2% related with BCD effect as evaluated in this study. We only changed albedo settings and all the input data and other parameters were the same as those in Fujita (2007) and Fujita et al. (2007). In the experiments, forcing albedo reductions means that homogeneous mixture of BC at glacier surface always reduce snow surface albedo of 2.0–5.2% compared to the control (density-based albedos). Runoff amount changes are due to surface albedo changes in the experiments. Total runoff amount

means the sum of runoff for 1 year from 10 October 1992.

The obtained results show a corresponding increase in total annual runoff from 70 to 204 mm of water equivalent by melt water from the glacier especially due to the June-August melting (melting season) (Fig. 8). In this study, we considered the case that the dark snow layer due to BC depositions during pre-monsoon season simply continues after pre-monsoon season. Thus, if the albedo reductions of 2.0–5.2% continues after the pre-monsoon season, the total runoff increases due to albedo changes corresponds to 11.6–33.9% of annual discharge of the Tibetan glacier. It is based on the comparison of the annual runoff amount roughly estimated from the difference between annual precipitation of 672 mm (observed) and evaporation of 70 mm (calculated) (Fujita and Ageta, 2000) with the calculated total increases of runoff amount due to the albedo reductions. Moreover, the acceleration of ablation processes in pre-monsoon season can cause the complete melting of snow cover and an advance in ice exposure to the solar radiation, with an additional reduction of surface albedo and more discharge.

Over Dongkemadi Glacier, air temperature begin to rise above freezing after June (Fujita et al., 2007), corresponding to the period of onset of monsoon. Hence, the effect of the albedo reductions on runoff increase appears after June. In our numerical tests, albedo reductions in the transient period from pre-monsoon to monsoon equals to the darkening effect of snow surface due to the integration of BC depositions during pre-monsoon season (March–May). The albedo reductions before monsoon season should not actually affect runoff increase in the study by Fujita (2007) because precipitation fallen in the succeeding monsoon season covered the darkened surface. However, if global warming expands the period of melting season in future, the albedo reductions during pre-monsoon will be important for increasing snow melt runoff from this glacier because of re-exposure of dirty surface by BC to the snow surface as indicated in Fujita (2007). In addition, rainfall below equilibrium line may sometimes contribute to re-exposures of BC layer to the surface with albedo reductions. Combination of upper and lower snow layer due to snow meltings, and additional BC depositions by

T. J. Yasunari et al.

wet deposition may also contribute to snow surface albedo reductions during monsoon season. However, quantitative discussions including all these effects are out of the scope of this study. In addition, BC flushing effect due to snow melting as discussed in Conway et al. (1996) and Flanner et al. (2007) may also be important for determining albedo reduction at the snow surface.

Due to the different locations, caution should be exercised in applying NCO-P results to other mountain sites. However some hints about the sensitivities of these albedo reductions on snowmelt runoff can be provided by this work. As we mentioned above, our estimation of snow contamination due to BCD and thus albedo reduction range, probably represents a lower estimate. Of course, this is the first step to estimate the BCD amount in the vicinity of NCO-P site and its concentration in surface snow in Himalayan region. Actually, more increase of snow melt can probably occur due to other atmospheric processes, snow aging, and additional mineral dust deposition. For better elucidating these processes, much observations and model studies for BC and dust deposition onto Himalayan regions and their effects on snow albedo feedback are needed.

4 Conclusions

We estimated a BCD amount of $266\,\mu g\,m^{-2}$ (=$2.89\,\mu g\,m^{-2}\,day^{-1}$) from dry deposition during pre-monsoon season over a Himalayan glacier at similar altitude of NCO-P site. Assuming the BCD is distributed uniformly on a pure 2-cm surface snow layer, we estimated BCC of 26.0–$68.2\,\mu g\,kg^{-1}$ within the range of the density at Yala glacier, which is in good agreement with the observations from southwestern China's glaciers. Hence, our estimated BCC range is considered to be realistic as lower bound BCC level at southern slopes of Himalayas. Assuming that the BCC range in snow is also representative near NCO-P and estimating albedo reductions by the BCC, the decreases of surface snow albedo of 2.0–5.2% were expected. If we assume these albedo reductions continues throughout the year, a possible 70–204 mm of water equivalent runoff

Full Screen / Esc

increase from a typical Tibetan glacier was found from simple model experiments. It represents a significant amount of the annual drainage from the glacier. Our results are applicable to white glaciers only (not for debris cover glacier). However, the estimate is likely to represent a lower bound for snow albedo reductions, since atmospheric wind and turbulence effects, snow aging, dust deposition, and snow albedo feedbacks were not considered. When all these processes are included, the actual snow albedo reduction in Himalayan glaciers is likely to be higher with more consequences on surface water runoffs from snow-ice melting. For these reasons we need more observations of BCC and BCD in Himalayan regions and better estimation of albedo reductions with better information of snow physical parameters in the regions by satellite and model studies in near future for assessing snow albedo feedbacks and accompanied snow melt runoff from glaciers.

Finally, we would like to further suggest the following additional things as guideline of future works on BC and dust impact on Himalayan and Tibetan glaciers. Still we need much more direct observations of BC and dust on deposition and concentration in snow surface over Himalayan and Tibetan regions to discuss precise impurity effects on albedo reductions. To know the mixture state of impurity in snow, it is important to carry out more detailed studies on dilution and enrichment effects of BC and dust by precipitation, snow surface melting, and combination between the snow surface layer and the snow layer below the snow surface, including the wet depositions of BC and dusts and flushing by melt water and precipitation. Although BC and dust can reduce snow surface albedos, we should know the equilibrium albedo reductions in the mixture of the impurities. Namely, we need to discuss the maximal albedo reductions due to BC and dust depositions. High-resolution regional and global models with realistic high-mountain snow-pack physics are also very helpful to understand the albedo reductions, and related snow processes all over Himalayan and Tibetan regions.

References

Aoki, Te., Aoki, Ta., Fukabori, M., Hachikubo, A., Tachibana, Y., and Nishio, F.: Effects of snow physical parameters on spectral albedo and bidirectional reflectance of snow surface, J. Geophys. Res., 105(D8), 10219–10236, 2000.

Aoki, Te., Motoyoshi, H., Kodama, Y., Yasunari, T. J., Sugiura, K., and Kobayashi, H.: Atmospheric aerosol deposition on snow surfaces and its effect on albedo, Sci. Online Lett. Atmos., 2, 13–16, doi:10.2151/sola.2006-004, 2006.

Aoki, Te., Motoyoshi, H., Kodama, Y., Yasunari, T. J., and Sugiura, K.: Variations of the snow physical parameters and their effects on albedo in Sapporo, Japan, Ann. Glaciol., 46, 375–381, 2007.

Bollasina, M., Bertolani, L., and Tartari, G.: Meteorological observations at high altitude in the Khumbu Valley, Nepal Himalayas, 1994–1999, Bull. Glaciol. Res., 19, 1–11, 2002.

Bonasoni, P., Laj, P., Angelini, F., Arduini, J., Bonafè, U., Calzolari, F., Cristofanelli, P., Decesari, S., Facchini, M. C., Fuzzi, S., Gobbi, G. P., Maione, M., Marinoni, A., Petzold, A., Roccato, F., Roger, J. C., Sellegri, K., Sprenger, M., Venzac, H., Verza, G. P., Villani, P., and Vuillermoz, E.: The ABC-Pyramid Atmospheric Research Observatory in Himalaya for aerosol, ozone and halocarbon measurements, Sci. Total Environ., 391(2–3), 252–261, 2008.

Bonasoni, P., Laj, P., Marinoni, A., Sprenger, M., Angelini, F., Arduini, J., Bonafè, U., Calzolari, F., Colombo, T., Decesari, S., Di Biagio, C., di Sarra, A. G., Evangelisti, F., Duchi, R., Facchini, M. C., Fuzzi, S., Gobbi, G. P., Maione, M., Panday, A., Roccato, F., Sellegri, K., Venzac, H., Verza, G. P., Villani, P., Vuillermoz, E., and Cristofanelli, P.: Atmospheric Brown Clouds in the Himalayas: first two years of continuous observations at the Nepal-Climate Observatory at Pyramid (5079 m), Atmos. Chem. Phys. Discuss., 10, 4823–4885, 2010, http://www.atmos-chem-phys-discuss.net/10/4823/2010/.

Cong, Z., Kang, S., and Qin, D.: Seasonal features of aerosol particles recorded in snow

from Mt. Qomolangma (Everest) and their environmental implications, J. Environ. Sci., 21(7), 914–919, 2009.

Cong, Z., Kang, S., Dong, S., Liu, X., and Qin, D.: Elemental and individual particle analysis of atmospheric aerosols from high Himalayas, Environ. Monit. Assess., 160, 323–335, doi:10.1007/s10661-008-0698-3, 2010.

Conway, H., Gades, A., and Raymond, C. F.: Albedo of dirty snow during conditions of melt, Water Resour. Res., 32(6), 1713–1718, 1996.

Decesari, S., Facchini, M. C., Carbone, C., Giulianelli, L., Rinaldi, M., Finessi, E., Fuzzi, S., Marinoni, A., Cristofanelli, P., Duchi, R., Bonasoni, P., Vuillermoz, E., Cozic, J., Jaffrezo, J. L., and Laj, P.: Chemical composition of PM_{10} and PM_1 at the high-altitude Himalayan station Nepal Climate Observatory-Pyramid (NCO-P) (5079 m a.s.l.), Atmos. Chem. Phys. Discuss., 9, 25487–25522, 2009,
http://www.atmos-chem-phys-discuss.net/9/25487/2009/.

Flanner, M. G., Zender, C. S., Randerson, J. T., and Rasch, P. J.: Present-day climate forcing and response from black carbon in snow, J. Geophys. Res., 112(D11), D11202, doi:10.1029/2006JD008003, 2007.

Flanner, M. G., Zender, C. S., Hess, P. G., Mahowald, N. M., Painter, T. H., Ramanathan, V., and Rasch, P. J.: Springtime warming and reduced snow cover from carbonaceous particles, Atmos. Chem. Phys., 9, 2481–2497, 2009,
http://www.atmos-chem-phys.net/9/2481/2009/.

Fujita, K., Takeuchi, N., and Seko, K.: Glaciological observations of Yala Glacier in Langtang Valley, Nepal Himalayas, 1994 and 1996, Bull. Glaciol. Res., 16, 75–81, 1998.

Fujita, K. and Ageta, Y.: Effect of summer accumulation on glacier mass balance on the Tibetan Plateau revealed by mass-balance model, J. Glaciol., 46, 244–252, 2000.

Fujita, K.: Effect of dust event timing on glacier runoff: sensitivity analysis for a Tibetan glacier, Hydrol. Process., 21(21), 2892–2896, 2007.

Fujita, K., Ohta, T., and Ageta, Y.: Characteristics and climatic sensitivities of runoff from a cold-type glacier on the Tibetan Plateau, Hydrol. Process., 21(21), 2882–2891, 2007.

Grenfell, T. C., Warren, S. G., and Mullen, P. C.: Reflection of Solar-Radiation by the Antarctic Snow Surface at Ultraviolet, Visible, and near-Infrared Wavelengths, J. Geophys. Res., 99(D9), 18669–18684, 1994.

Hadley, O. L., Ramanathan, V., Carmichael, G. R., Tang, Y., Corrigan, C. E., Roberts, G. C., and Mauger, G. S.: Trans-Pacific transport of black carbon and fine aerosols ($D < 2.5\,\mu m$) into

Estimated lower bound BC deposition over Himalayas

T. J. Yasunari et al.

Title Page

Abstract	Introduction
Conclusions	References
Tables	Figures

|◄|►|

◄ | ►

Back | Close

Full Screen / Esc

Printer-friendly Version

Interactive Discussion

North America, J. Geophys. Res., 112(D5), D05309, doi:10.1029/02006JD007632, 2007.

Han, Z. W., Ueda, H., Matsuda, K., Zhang, R. J., Arao, K., Kanai, Y., and Hasome, H.: Model study on particle size segregation and deposition during Asian dust events in March 2002, J. Geophys. Res., 109(D19), D19205, doi:10.1029/12004JD004920, 2004.

Hansen, J. and Nazarenko, L.: Soot climate forcing via snow and ice albedos, Proc. Natl. Acad. Sci. USA, 101(2), 423–428, 2004.

Holland, D. M.: Merged IBCAO/ETOPO5 Global Topographic Data Product. National Geophysical Data Center (NGDC), Boulder Colorado, 2000, http://fish.cims.nyu.edu/project_aomip/forcing_data/topography/merged/overview.html.

IPCC: Summary for Policymakers, in: Climate Change 2007: The Physical Science Basis. Contribution of Working Group I to the Fourth Assessment Report of the Intergovernmental Panel on Climate Change, edited by: Solomon, S., Qin, D., Manning, M., Chen, Z., Marquis, M., Averyt, K. B.,Tignor, M., and Miller, H. L., Cambridge University Press, Cambridge, United Kingdom and New York, NY, USA, 2007.

Jacobson, M. Z.: Climate response of fossil fuel and biofuel soot, accounting for soot's feedback to snow and sea ice albedo and emissivity, J. Geophys. Res., 109, D21201, doi:10.1029/2004JD004945, 2004.

Karma, Ageta, Y., Naito, N., Iwata, S., and Yabuki, H.: Glacier distribution in the Himalayas and glacier shrinkage from 1963 to 1993 in the Bhutan Himalayas, Bull. Glaciol. Res., 20, 29–40, 2003.

Lau, K. M., Kim, M. K., and Kim, K. M.: Asian summer monsoon anomalies induced by aerosol direct forcing: the role of the Tibetan Plateau, Clim. Dynam., 26(7–8), 855–864, 2006.

Lau, K. M., Ramanathan, V., Wu, G.-X., Li, Z., Tsay, S. C., Hsu, C., Sikka, R., Holben, B., Lu., D., Tartari, G., Chin, M., Koudelova, P., Chen, H., Ma, Y., Huang, J., Taniguchi, K., and Zhang, R.: The Joint Aerosol-Monsoon Experiment – A new challenge for monsoon climate research, Bull. Amer. Meteorol. Soc., 89(1), 369–383, doi:10.1175/BAMS-89-3-369, 2008.

Lau, K. M., Kim, M. K., and Kim, K. M.: Enhanced surface warming and snow melt in the Himalayas and Tibetan Plateau induced by the EHP effect, Environ. Res. Lett., 5, 025204, doi:10.1088/1748-9326/5/2/025204, 2010.

Lindstedt, P. R.: Simplified soot nucleation and surface growth steps for non-premixed flame, in: Soot Formation in Combustion: Mechanisms and Models, edited by: Bockhorn, H., Springer-Verlag, Berlin, 417–41, 1994.

Marcq, S., Laj, P., Roger, J. C., Villani, P., Sellegri, K., Bonasoni, P., Marinoni, A., Cristo-

Estimated lower bound BC deposition over Himalayas

T. J. Yasunari et al.

Title Page

Abstract	Introduction
Conclusions	References
Tables	Figures

⏮   ⏭

◀   ▶

Back   Close

Full Screen / Esc

Printer-friendly Version

Interactive Discussion

fanelli, P., Verza, G. P., and Bergin, M.: Aerosol optical properties and radiative forcing in the high Himalaya based on measurements at the Nepal Climate Observatory-Pyramid site (5100 m a.s.l), Atmos. Chem. Phys. Discuss., 10, 5627–5663, 2010, http://www.atmos-chem-phys-discuss.net/10/5627/2010/.

Marinoni, A., Cristofanelli, P., Laj, P., Duchi, R., Calzolari, F., Decesari, S., Sellegri, K., Vuillermoz, E., Verza, G. P., Villani, P., and Bonasoni, P.: Aerosol mass and black carbon concentrations, two year-round observations at NCO-P (5079 m, Southern Himalayas), Atmos. Chem. Phys. Discuss., 10, 8379–8413, 2010, http://www.atmos-chem-phys-discuss.net/10/8379/2010/.

Ming, J., Cachier, H., Xiao, C., Qin, D., Kang, S., Hou, S., and Xu, J.: Black carbon record based on a shallow Himalayan ice core and its climatic implications, Atmos. Chem. Phys., 8, 1343–1352, 2008, http://www.atmos-chem-phys.net/8/1343/2008/.

Ming, J., Xiao, C., Cachier, H., Qin, D., Qin, X., Li, Z., and Pu, J.: Black Carbon (BC) in the snow of glaciers in west China and its potential effects on albedos, Atmos. Res., 92(1), 114–123, 2009.

Nho-Kim, E.-Y., Michou, M., and Peuch, V.-H.: Parameterization of size-dependent particle dry deposition velocities for global modeling, Atmos. Environ., 38, 1933–1942, 2004.

Petzold, A., Kramer, H., and Schönlinner, M.: Continuous measurement of atmospheric black carbon using a Multi-Angle Absorption Photometer, Environ. Sci. Pollut. Res., 4, 78–82, 2002.

Ramanathan, V., Li, F., Ramana, M. V., Praveen, P. S., Kim, D., Corrigan, C. E., Nguyen, H., Stone, E. A., Schauer, J. J., Carmichael, G. R., Adhikary, B., and Yoon, S. C.: Atmospheric brown clouds: Hemispherical and regional variations in long-range transport, absorption, and radiative forcing, J. Geophys. Res., 112, D22S21, doi:10.1029/2006JD008124, 2007.

Tanikawa T., Stamnes K., Aoki T., Kuchiki K., Hachikubo A., and Sugiura K.: Effect of snow impurities and vertical profile on snow albedo and reflectance, Eos Trans. AGU, 90(52), Fall Meet. Suppl., Abstract C33C-0519, 2009.

Uno, I., Eguchi, K., Yumimoto, K., Takemura, T., Shimizu, A., Uematsu, M., Liu, Z., Wang, Z., Hara, Y., and Sugimoto, N.: Asian dust transported one full circuit around the globe, Nature Geoscience, 2, 557–560, doi:10.1038/NGEO583, 2009.

Venzac, H., Sellegri, K., Laj, P., Villani, P., Bonasoni, P., Marinoni, A., Cristofanelli, P., Calzolari, F., Fuzzi, S., Decesari, S., Facchini, M.-C., Vuillermoz, E., and Verza, G. P.: High frequency

Estimated lower bound BC deposition over Himalayas

T. J. Yasunari et al.

Title Page

Abstract | Introduction

Conclusions | References

Tables | Figures

◄ | ►

◄ | ►

Back | Close

Full Screen / Esc

Printer-friendly Version

Interactive Discussion

new particle formation in the Himalayas, Proc. Natl. Acad. Sci. USA, 105(41), 15666–15671, 2008.

Warren, S. G. and Wiscombe, W. J.: A Model for the Spectral Albedo of Snow 2. Snow Containing Atmospheric Aerosols, J. Atmos. Sci., 37(12), 2734–2745, 1980.

Warren, S. G. and Wiscombe, W. J.: Dirty snow after nuclear war, Nature, 313, 467–470, 1985.

Xu, B., Yao, T., Liu, X., and Wang, N.: Elemental and organic carbon measurements with a two-step heating-gas chromatography system in snow samples from the Tibetan Plateau, Ann. Glaciol., 43, 257–262, 2006.

Xu, B., Wang, M., Joswiak, D. R., Cao, J., Yao, T., Wu, G., Yang, W., and Zhao, H.: Deposition of anthropogenic aerosols in a southeastern Tibetan glacier, J. Geophys. Res., 114, D17209, doi:10.1029/2008JD011510, 2009a.

Xu, B., Cao, J., Hansen, J., Yao, T., Joswiak, D. R., Wang, N., Wu, G., Wang, M., Zhao, H., Yang, W., Liu, X., and He, J.: Black soot and the survival of Tibetan glaciers, Proc. Natl. Acad. Sci. USA, 106(52), 22114–22118, doi:10.1073/pnas.0910444106, 2009b.

Yamazaki, T., Kondo, J., Sakuraoka, T., and Nakamura, T.: A one-dimensional model of the evolution of snow-cover characteristics, Ann. Glaciol., 18, 22–26, 1993.

Yasunari, T. J. and Yamazaki, K.: Impacts of Asian dust storm associated with the stratosphere-to-troposphere transport in the spring of 2001 and 2002 on dust and tritium variations in Mount Wrangell ice core, Alaska, Atmos. Environ., 43, 2582–2590, doi:10.1016/j.atmosenv.2009.02.025, 2009.

Title Page

Abstract | Introduction

Conclusions | References

Tables | Figures

◄ | ►

◄ | ►

Back | Close

Full Screen / Esc

Printer-friendly Version

Interactive Discussion

Table 1. Surface snow density at Yala glacier (5450 m).

Date	Depth (cm)	ρ (kg m^{-3})
1996/5/20	3	320
1996/6/23	5	512
1996/6/27	3	338
1996/7/28	3	468
1996/8/3	7	426
1996/8/3	2	413
1996/8/23	5	389
1996/8/31	2.5	357
1996/10/9	5	195

Table 2. Comparison between estimated (a) and observed (b, c, d, e, f) BCCs in snow and ice core for locations reported in Fig. 1.

Site in Himalayan region	Altitude (m)	BCCs in snow and ice core ($\mu g\,kg^{-1}$)
NCO-P (lat. 27.958, lon. 86.815)[a]	5079	26.0–68.2[e]
Qiangyong Glacier (lat. 28.83, lon. 90.25)[b]	5400	43.1
Kangwure Glacier (lat. 28.47, lon. 85.82)[b]	6000	21.8
East Rongbuk Glacier (lat. 28.02, lon. 86.96)[c]	6465	18.0
East Rongbuk Glacier (lat. 28.02, lon. 86.96)[d]	6500	20.3±9.2

[a] This work. [b] The EC concentration data in snow sample by Xu et al. (2006). [c] The BCC data in snow sample by Ming et al. (2009). [d] The BCC data during 1995–2002 in an ice core by Ming et al. (2008). The BCC exceeded $50\,\mu g\,kg^{-1}$ in the summer of 2001. [e] Estimated BCC in 2-cm surface snow with density variations of 195–$512\,kg\,m^{-3}$ at Yala Glacier (see, Fig. 1).

Table 3. Regression equations of each mixture state of BC and snow type.

Mixture State	Snow type	Regression equation	R^2	N	σy [%]
External	New snow	Eq. (1) $y = -8.08653E - 05x^2 + 4.79226E - 02x + 2.97897E - 01$	0.99	14	0.18
	Old Snow	Eq. (2) $y = 1.51204E - 01x + 6.85961E - 01$	0.98	10	0.49
Internal	New snow	Eq. (3) $y = -1.20051E - 04x^2 + 6.94225E - 02x + 6.59244E - 01$	0.98	14	0.45
	Old Snow	Eq. (4) $y = 2.20386E - 01x + 1.51181$	0.96	10	1.06

Table 4. Possible albedo reductions by different equations on the relationship between BC concentration and reduced albedo.

Equations	Surface snow density [kg m^{-3}]	Reduced albedo [%]
Eq. by Ming et al. (2009)	195	5.2
	512	2.0
Eq. (1)[a]	195	3.2
	512	1.5
Eq. (2)[a]	195	11.0
	512	4.6
Eq. (3)[a]	195	4.8
	512	2.4
Eq. (4)[a]	195	16.5
	512	7.2

[a] Equations from Table 3 were used for estimating possible albedo reductions.

Title Page

Abstract   Introduction

Conclusions   References

Tables   Figures

◄◄   ►►

◄   ►

Back   Close

Full Screen / Esc

Printer-friendly Version

Interactive Discussion
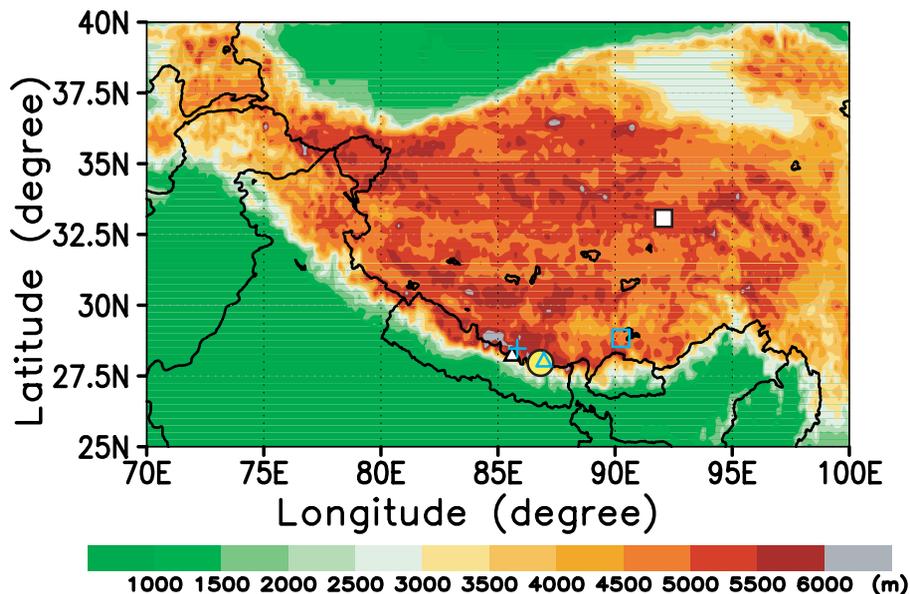
Fig. 1. Location map of research sites focused in this study. The large circle in yellow denote NCO-P site. The triangle and square in white colour denote Yala Glacier, and Dongkemadi Glacier, respectively. The cross, triangle, and square in sky blue denote the locations of Kangwure Glacier, East Rongbuk Glacier, and Qiangyong Glacier, respectively, where BC concentrations in snow were measured by Xu et al. (2006) and Ming et al. (2008, 2009). The Merged IBCAO/ETOPO5 Global Topographic Data Product by Holland (2000) was used for topography map.
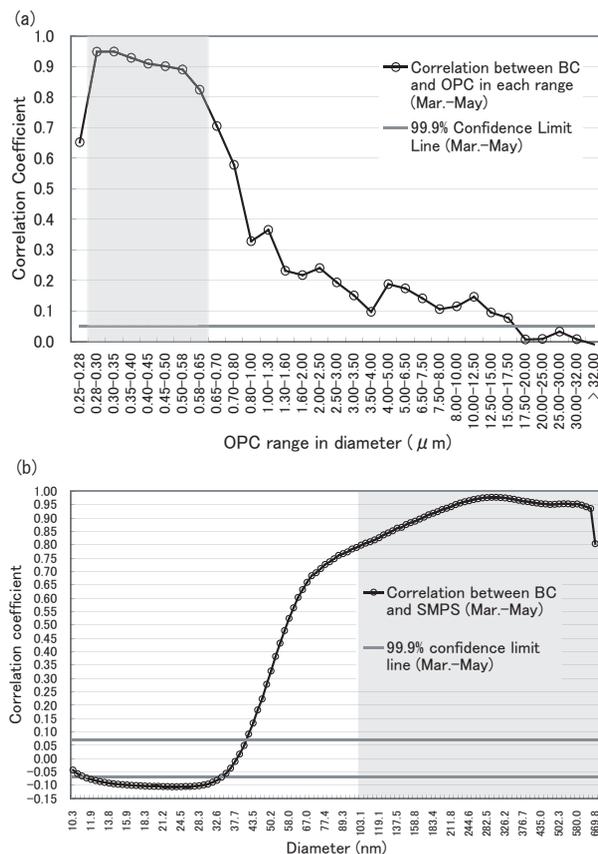
Fig. 2. Correlation coefficients (black solid line with circle) for March–May in time series data between atmospheric eqBCC and **(a)** particle counts in each size (as measured by OPC); **(b)** (as measured by SMPS). The bold line in gray denotes 99.9% confidence limit lines. The shade size ranges correspond to the correlation coefficient of more than 0.8.

Estimated lower bound BC deposition over Himalayas

T. J. Yasunari et al.

Title Page

Abstract | Introduction

Conclusions | References

Tables | Figures

|◄ | ►|

◄ | ►

Back | Close

Full Screen / Esc

Printer-friendly Version

Interactive Discussion
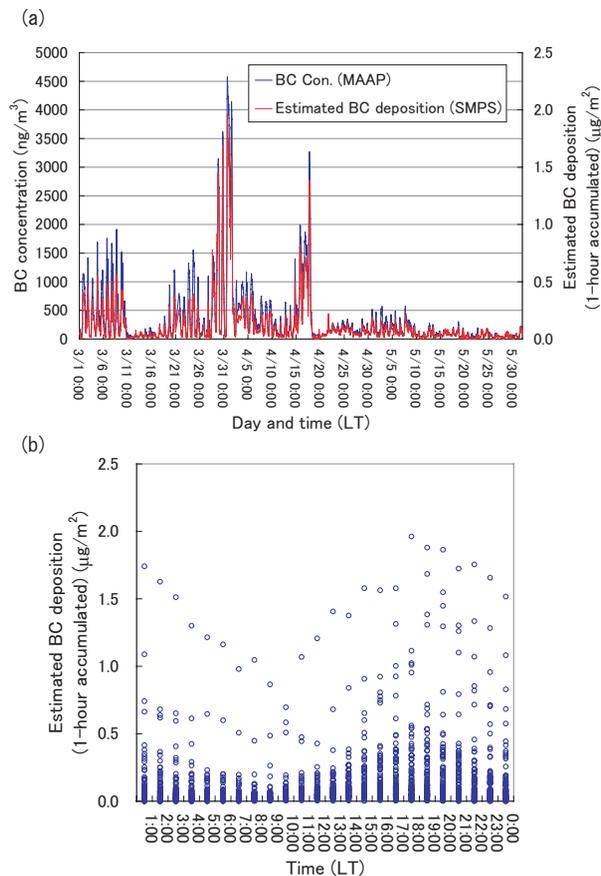
Fig. 3. **(a)** One-hour mean eqBCC from MAAP data (Bonasoni et al., 2008) and estimated hourly total BCD flux (right side scale) as multiplying dry deposition amount from SMPS data by 0.087 during March–May in 2006; **(b)** Composite of the estimated hourly total BCD flux during March–May in 2006.
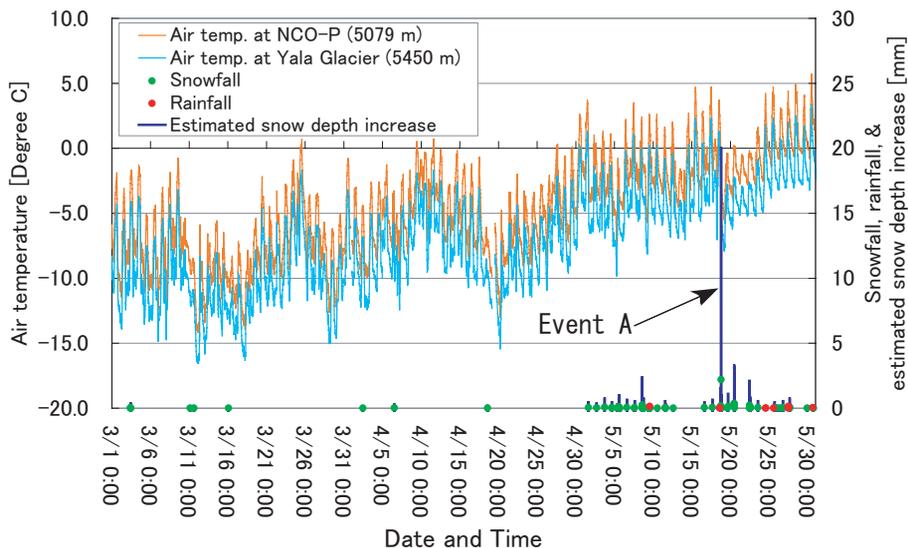
Fig. 4. Air temperature variations at NCO-P site and over Yala Glacier, together with the amount of snowfall and rainfall, and estimated snow depth increases over Yala Glacier. The air temperature over Yala Glacier was estimated with temperature lapse rate of $6.5\,\mathrm{K\,km^{-1}}$. If air temperature was below 0 degree in Celsius, precipitation was considered to be snow. The snow depth increases were calculated with a typical fresh snow density of $110\,\mathrm{kg\,m^{-3}}$.
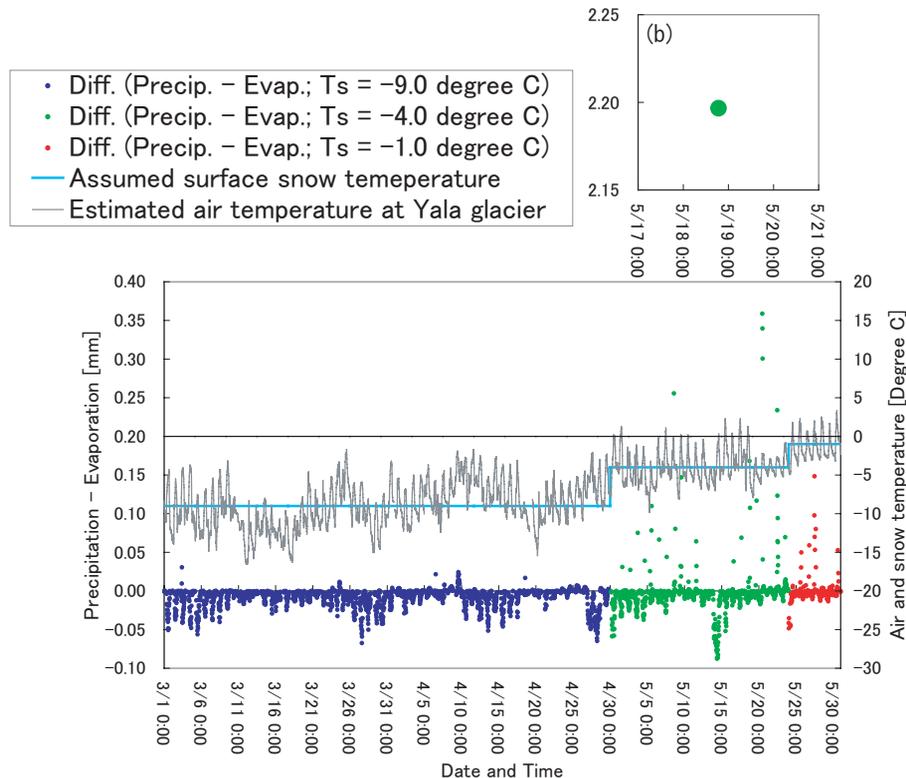
Fig. 5. Difference between precipitation (P) and estimated evaporation (E) (sublimation in this study). The constant snow surface temperatures of –9, –4, and –1° were used during 3/1–4/29, 4/30–5/23, and 5/24–5/31, respectively. One data in $P – E$ at the time of Event A was located at out of range and plotted in **(b)** separately. In (b), vertical and horizontal axes have the same units as **(a)**.
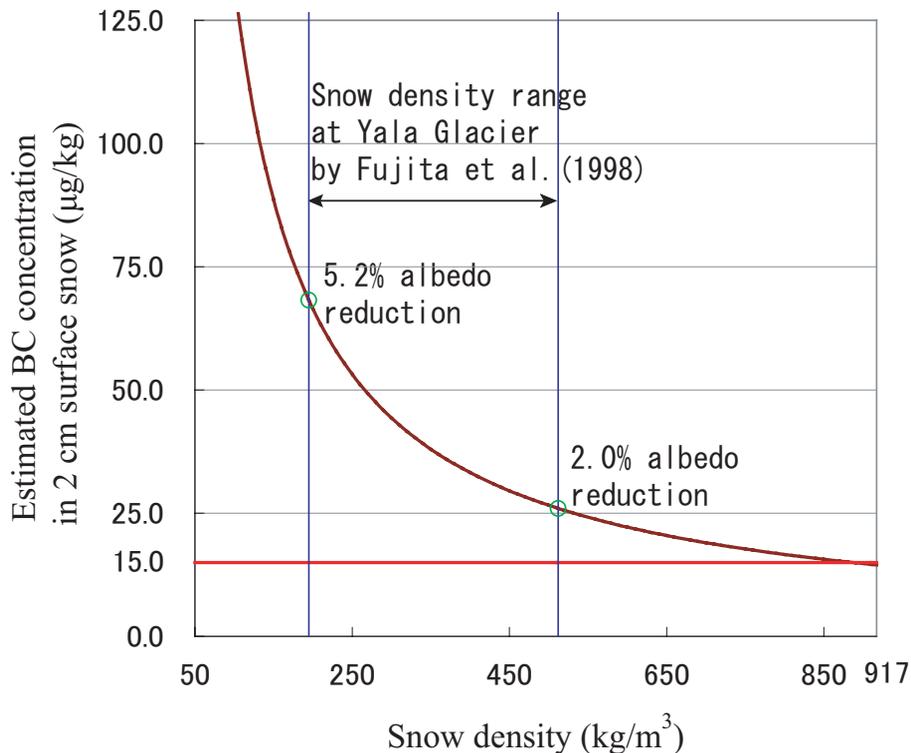
Fig. 6. The relationship between snow density and the calculated BCC in surface snow together with related albedo reductions. The brown curved and red lines denote the estimated BCD of 266 µg m^{-2} from NCO-P data and the 1% albedo reduction line by BCC of 15 µg kg^{-1} in snow mentioned in Grenfell et al. (1994) indicated by the calculations of Warren and Wiscombe (1980). The range between two blue solid lines corresponds to the range of snow density variations of 195–512 kg m^{-3} in surface snow at Yala glacier by Fujita et al. (1998). The green circles are estimated maximal and minimal albedo reductions due to BCC in snow by using a linear regression equation of Ming et al. (2009).

Title Page

Abstract | Introduction

Conclusions | References

Tables | Figures

◀ | ▶

◀ | ▶

Back | Close

Full Screen / Esc

Printer-friendly Version

Interactive Discussion
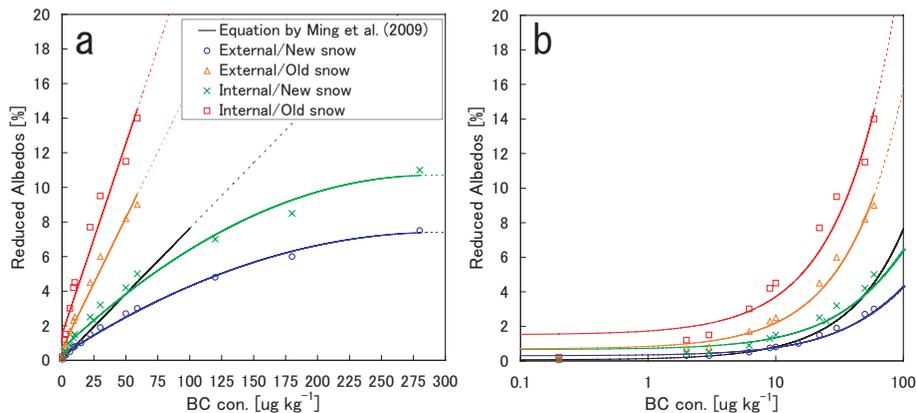
Fig. 7. Albedo reductions for 2 types of BC mixture conditions (external and internal mixture, called Ext and Int, respectively) with 2 types of snow conditions (new and old snow, called New and Old, respectively) together with the estimated albedo reductions by the equation of Ming et al. (2009). **(b)** denotes an enlarged **(a)** for the BC concentration range up to $100\,\mu g\,kg^{-1}$ with log scale for x-axis. The parts of dashed lines denote out of ranges of the employed data. If you use the data estimated from each equation in Table 3 on the part of dashed line for various studies, you should be careful for your discussions on albedo reductions because of no supporting observations in these ranges.

ACPD

10, 9291–9328, 2010

Estimated lower bound BC deposition over Himalayas

T. J. Yasunari et al.

Title Page

Abstract | Introduction

Conclusions | References

Tables | Figures

◄ | ►►

◄ | ►

Back | Close

Full Screen / Esc

Printer-friendly Version

Interactive Discussion
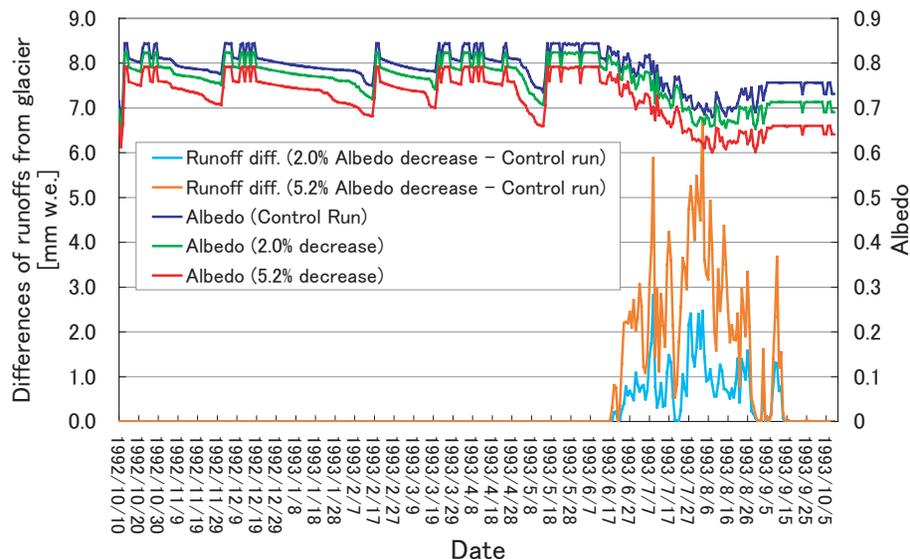
Fig. 8. Increases of snow melt runoff from Dongkemadi Glacier due to continuous albedo reductions of 2.0% and 5.2% in the numerical experiments. The lines in blue, green, and red denote the areal weighted mean of snow albedos along each altitude in the domain of Fujita (2007) and Fujita et al. (2007) for the cases of control run (no forced albedo reduction), 2.0% albedo reduction, and 5.2% albedo reduction, respectively. The lines in sky blue and orange denote the differences of snow melt runoff from the glacier between the cases of 2.0% albedo reduction and control run and between 5.2% albedo reduction and control run, respectively.